Supplementary materials

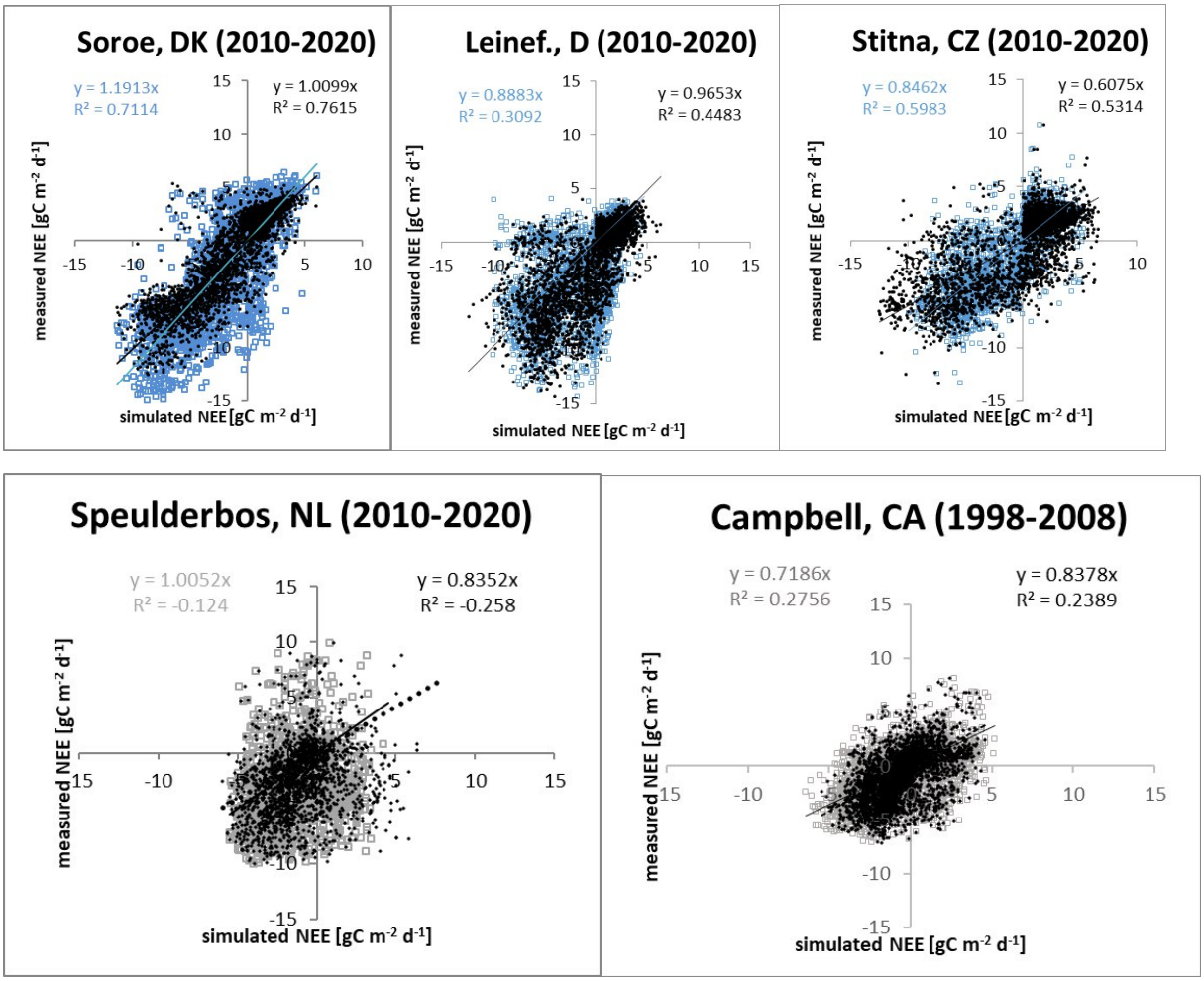

Fig. S1: Measured and simulated net carbon exchange of the ecosystem (NEE) at three beech and 2 Douglas fir ICOS sites. Black points: simulation with standard parameters, Black points: standard parameters, Blue/gray points site parameters, Blue rectangles: Beech, Gray rectangles: Douglas fir.

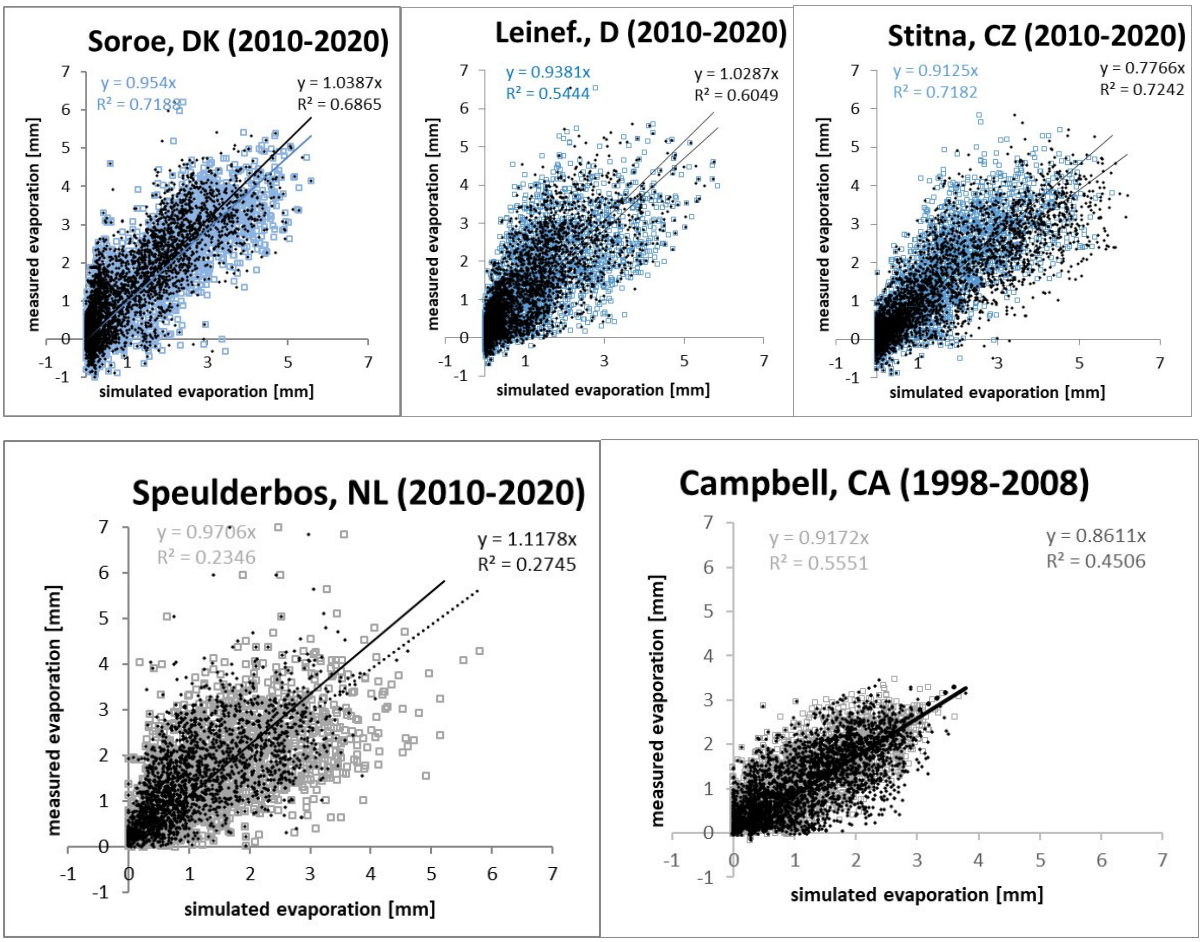

Fig. S2: Measured and simulated evaporation at three beech and 2 Douglas fir ICOS sites. Black points: simulation with standard parameters, Blue/gray points site parameters, Blue rectangles: Beech, Gray rectangles: Douglas fir.

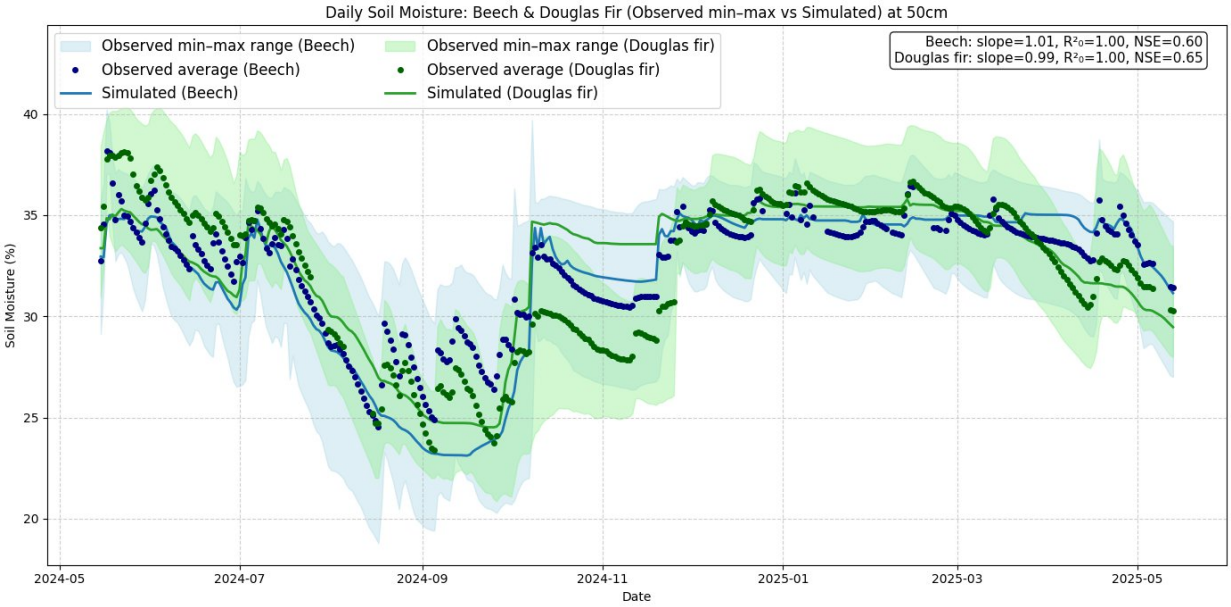

Fig. S3: Comparison of measured and simulated soil moisture at 50 cm depths in pure beech and pure Douglas fir plots from May 2024 to May 2025 at the ECOSENSE forest. Soil moisture was measured at five replicate points per depth in each plot. Simulated values are outputs of LandscapeDNDC model.

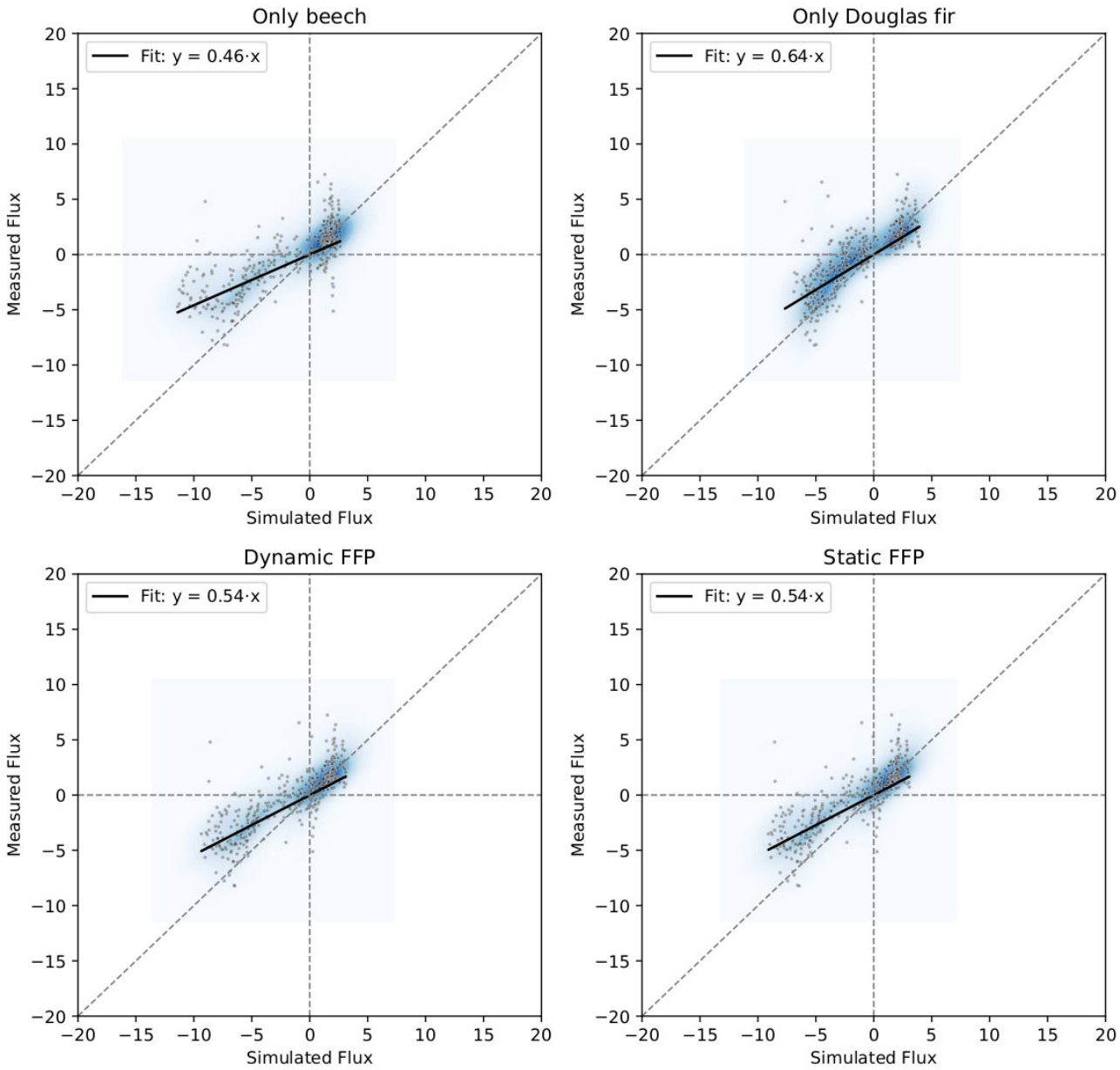

Fig. S4: Comparison between hourly measured and simulated net ecosystem exchange (NEE, kgC $ha^{-1}hr^{-1}$) during the flushing phase (April: early flushing phase) at the ECOSENSE forest. (a) Simulated NEE for a pure beech stand compared to measured eddy covariance (EC) NEE. (b) Simulated NEE for a pure Douglas fir stand compared to measured EC NEE. (c) Weighted NEE based on a dynamic footprint composition, with hourly contributions from each species estimated using footprint–land cover overlay. (d) Weighted NEE based on a static footprint composition (66.5% beech, 33.5% Douglas fir). The shaded heatmap represents the kernel density estimate of point concentrations (darker blue regions correspond to higher density).

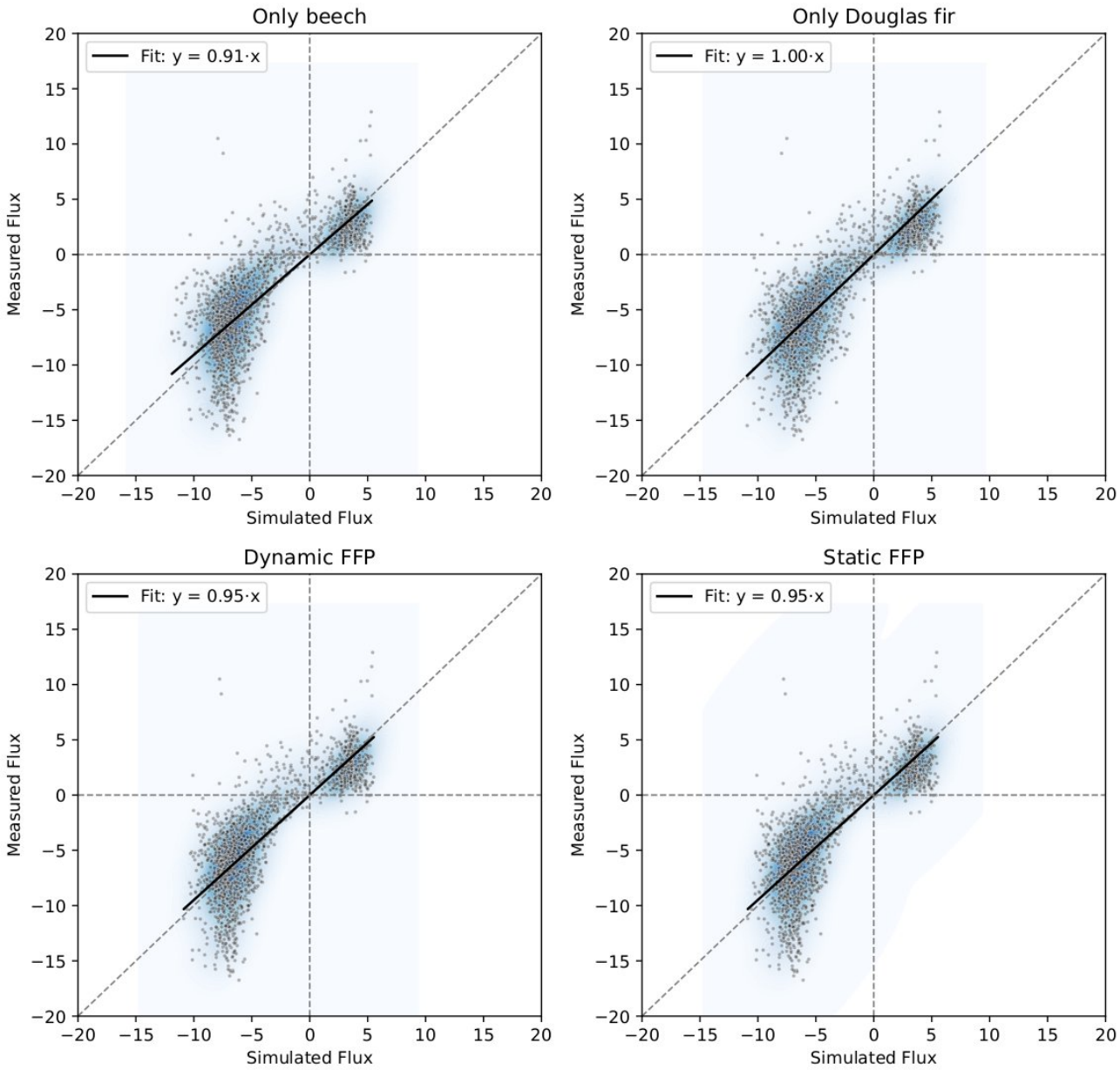

Fig. S5: Comparison between hourly measured and simulated net ecosystem exchange (NEE, kgC $ha^{-1}hr^{-1}$) during the peak growing season (May to September) at the ECOSENSE forest. (a) Simulated NEE for a pure beech stand compared to measured EC NEE. (b) Simulated NEE for a pure Douglas fir stand compared to measured EC NEE. (c) Weighted NEE based on a dynamic footprint composition, with hourly contributions from each species estimated using footprint–land cover overlay. (d) Weighted NEE based on a static footprint composition (66.5% beech, 33.5% Douglas fir). The shaded heatmap represents the kernel density estimate of point concentrations (darker blue regions correspond to higher density).

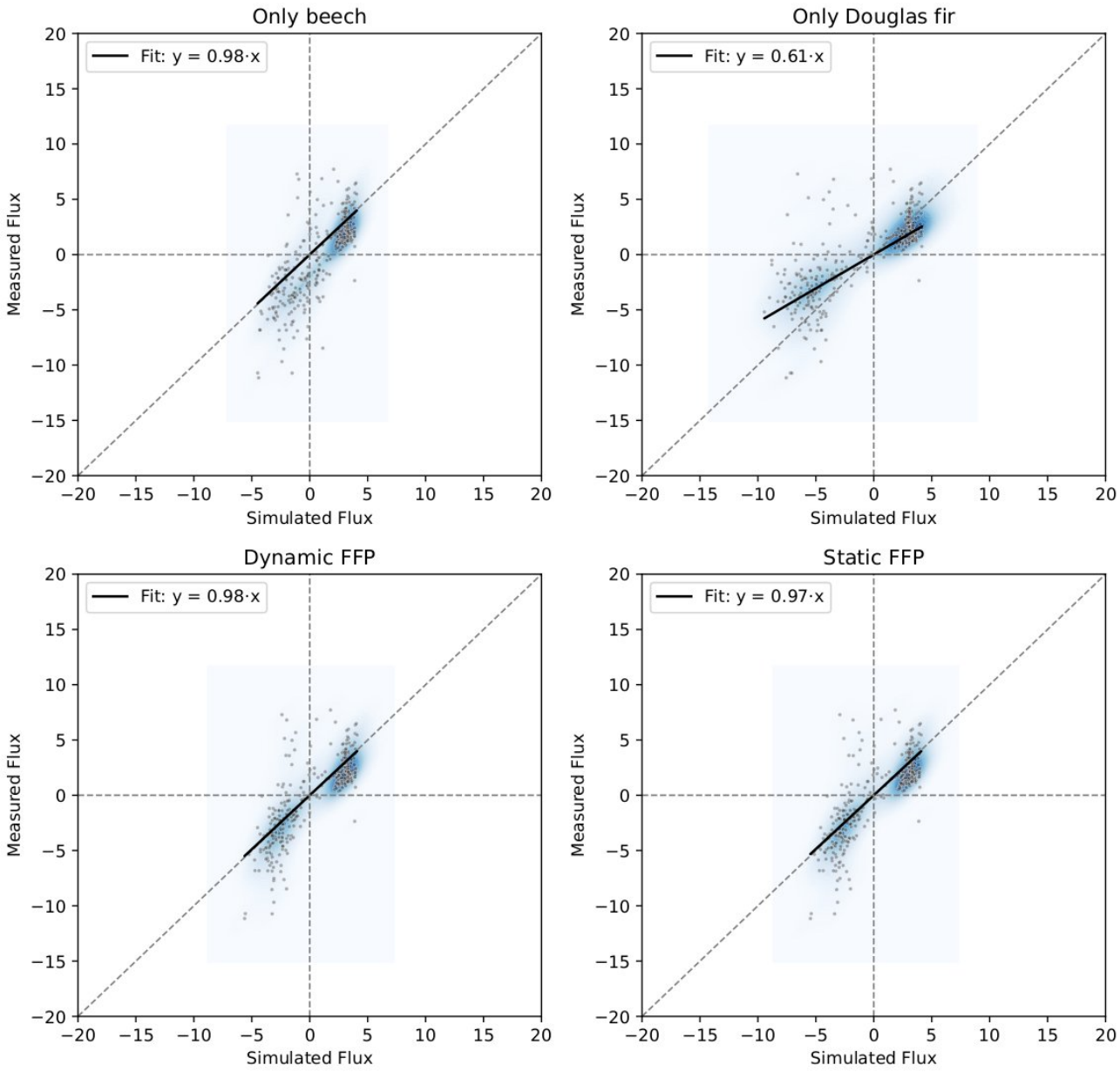

Fig. S6: Comparison between hourly measured and simulated net ecosystem exchange (NEE, kgC $ha^{-1}hr^{-1}$) during the senescence (October) at the ECOSENSE forest. (a) Simulated NEE for a pure beech stand compared to measured EC NEE. (b) Simulated NEE for a pure Douglas fir stand compared to measured EC NEE. (c) Weighted NEE based on a dynamic footprint composition, with hourly contributions from each species estimated using footprint–land cover overlay. (d) Weighted NEE based on a static footprint composition (66.5% beech, 33.5% Douglas fir). The shaded heatmap represents the kernel density estimate of point concentrations (darker blue regions correspond to higher density).

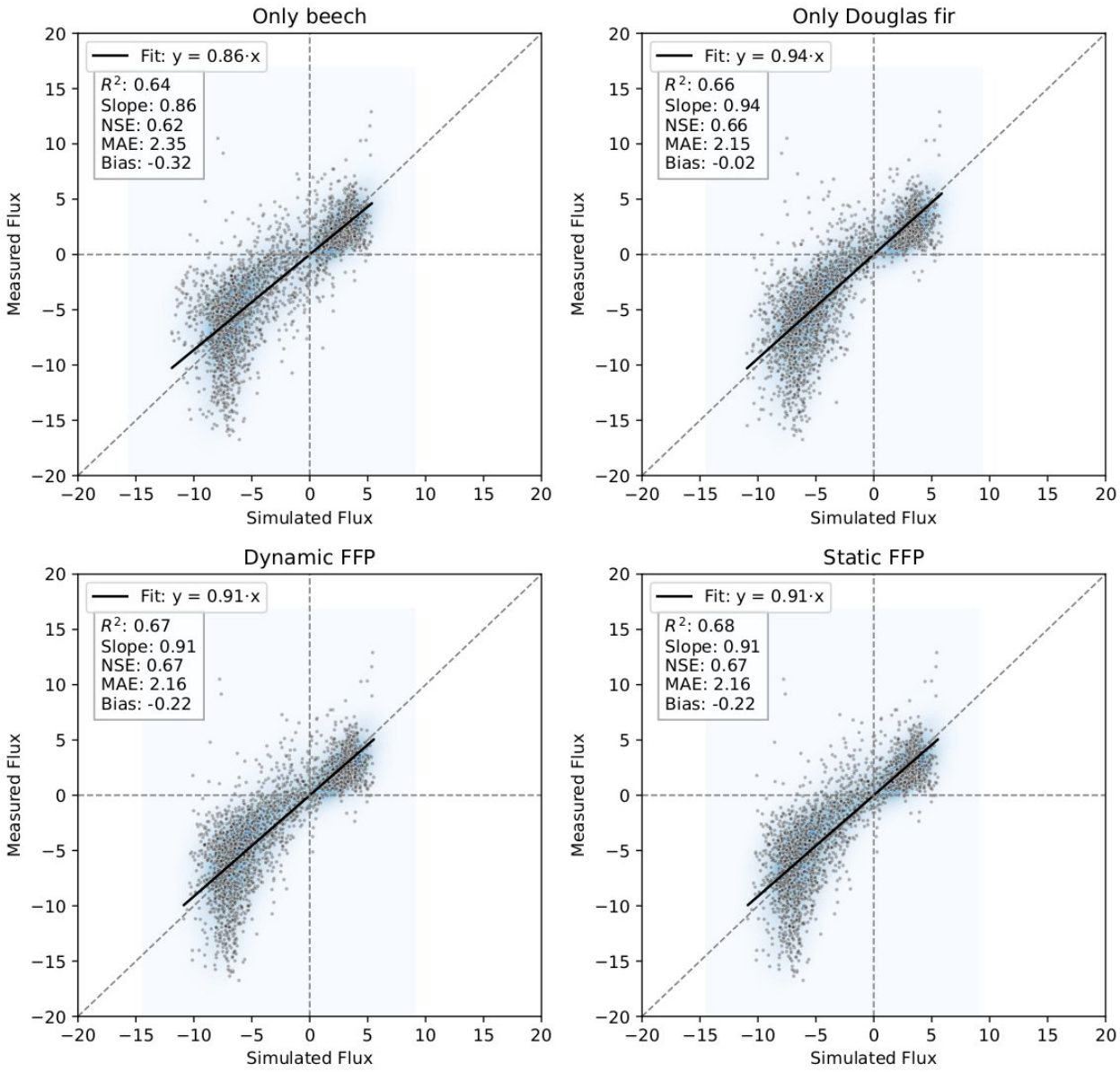

Fig. S7: Comparison between hourly measured and simulated net ecosystem exchange (NEE, kgC $ha^{-1}hr^{-1}$) during the growing season (April to October) at the ECOSENSE forest. (a) Simulated NEE for a pure beech stand compared to measured EC NEE. (b) Simulated NEE for a pure Douglas fir stand compared to measured EC NEE. (c) Weighted NEE based on a dynamic footprint composition, with hourly contributions from each species estimated using footprint–land cover overlay. (d) Weighted NEE based on a static footprint composition (66.5% beech, 33.5% Douglas fir). The shaded heatmap represents the kernel density estimate of point concentrations (darker blue regions correspond to higher density)

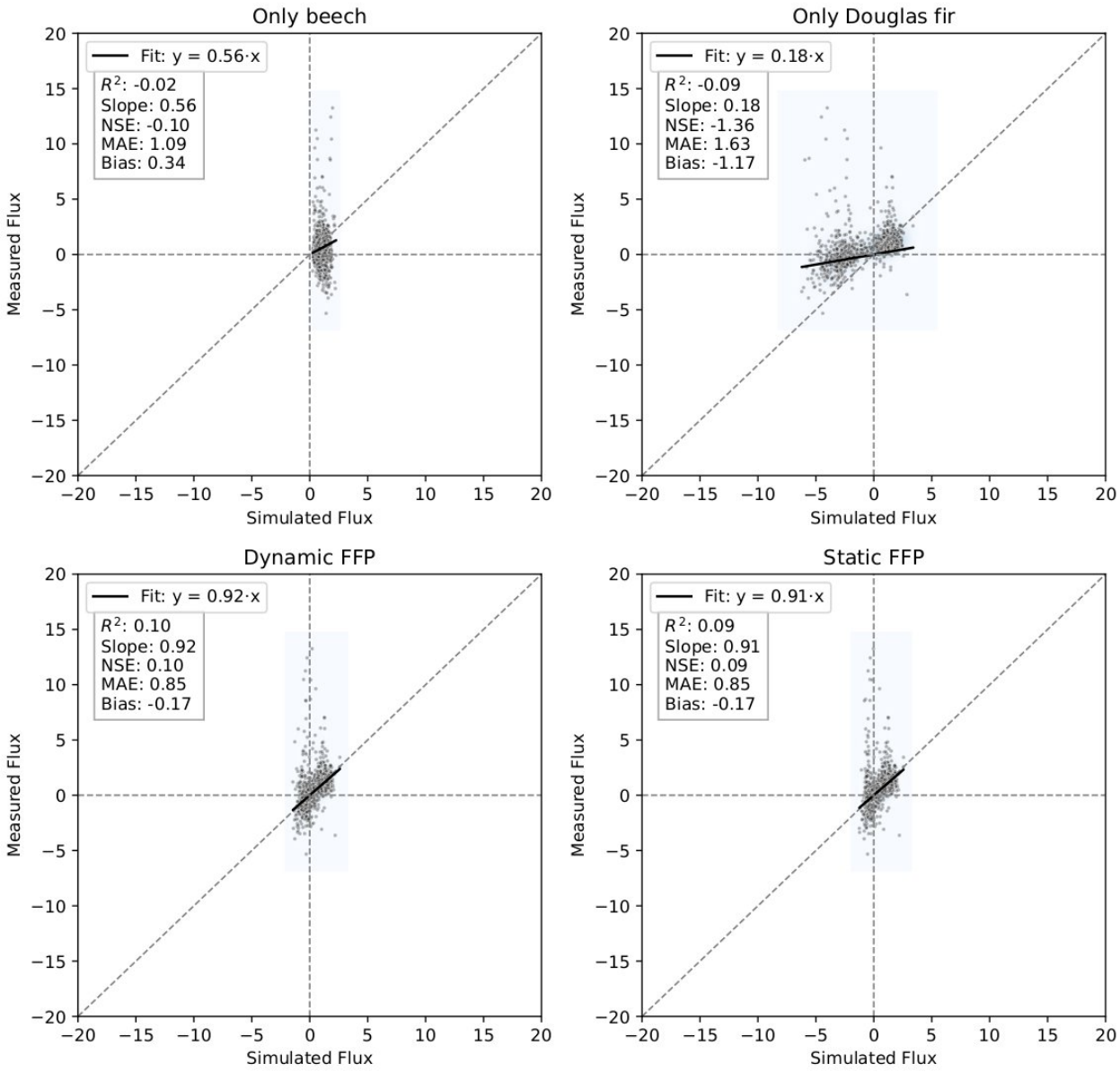

Fig. S8: Comparison between hourly measured and simulated net ecosystem exchange (NEE, kgC $ha^{-1}hr^{-1}$) during the growing season (November to March) at the ECOSENSE forest. (a) Simulated NEE for a pure beech stand compared to measured EC NEE. (b) Simulated NEE for a pure Douglas fir stand compared to measured EC NEE. (c) Weighted NEE based on a dynamic footprint composition, with hourly contributions from each species estimated using footprint–land cover overlay. (d) Weighted NEE based on a static footprint composition (66.5% beech, 33.5% Douglas fir). The shaded heatmap represents the kernel density estimate of point concentrations (darker blue regions correspond to higher density)

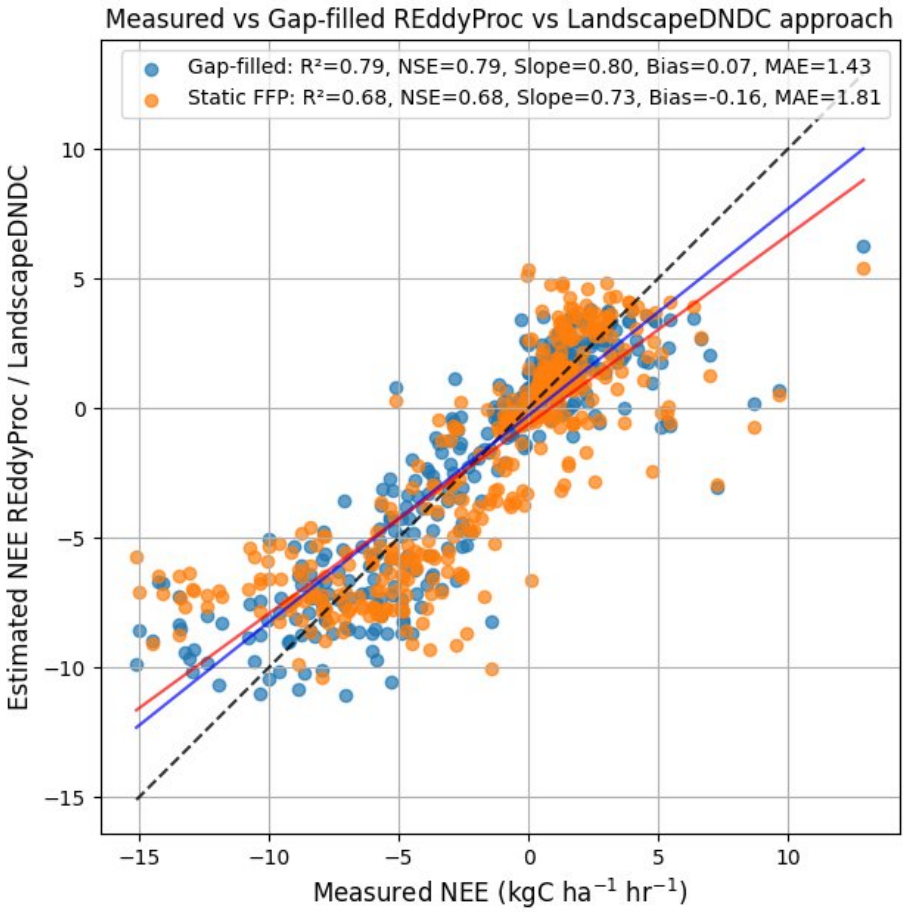

Fig. S9: Comparison between hourly measured and gap filled net ecosystem exchange (NEE, kgC $ha^{-1}hr^{-1}$) using the REddyProc and the process based LandscapeDNDC approach . We randomly created 627 artificial gaps in the measured data and filled them with the two approaches.

Table S1: Parameters affecting the simulation of carbon and water exchange by LandscapeDNDC model.

Variable	Description	Beech	Douglas fir	References (Beech; Douglas fir)
Photosynthesis				
AEKC	Activation energy for Michaelis-Menten constant for CO_2 (J mol^{-1})	65000	65000	Wang et al. (2003); Falge et al. (1997) (assumed similar to Norway spruce)
AEKO	Activation energy for Michaelis-Menten constant for O_2 (J mol^{-1})	36000	36000	Wang et al. (2003); Falge et al. (1997) (assumed similar to Norway spruce)
AERD	Activation energy for dark respiration (J mol^{-1})	36500	63500	Dreyer et al. (2001); Falge et al. (1997) (assumed similar to Norway spruce)
AEVC	Activation energy for photosynthesis (J mol^{-1})	70627	75750	Kattge and Knorr (2007); Falge et al. (1997) (assumed similar to Norway spruce)
AEVO	Activation energy for RubP oxygenation (J mol^{-1})	37530	37530	Long (1991) (all species)
AEJM	Activation energy for electron transport (J mol^{-1})	48090	40000	Medlyn et al. (2002); Ibrom et al. (2006) (assumed similar to Norway spruce)
KC25	Michaelis-Menten constant for CO_2	299.5	260.0	Wang et al. (2003); Von Caemmerer et al. (1994)
KO25	Michaelis-Menten constant for O_2	159.6	179.0	Wang et al. (2003); Von Caemmerer et al. (1994)
QVOVC	Relation between saturated rate of oxygenation and carboxylation	0.21	0.21	Long (1991) (all species)
QJVC	Relation between max. electron transport rate and RubP-saturated carboxylation	2.24	2.8	Yan et al. (2023); Manter et al. (2003)
QRD25	Relation between dark respiration rate and carboxylation capacity	0.0149	0.012	Yan et al. (2023); Warren and Adams (2006)
SLOPE_GSA	Slope of stomata response in the BERRY-BALL model	11.8	4.0	Dufrene et al. (2005); Van Wijk et al. (2000)
THETA	Curvature parameter for photosynthesis	0.882	0.9	Yan et al. (2023); Thornley (2002)
VCMAX25	Saturated rate of carboxylation at 25 °C (µmol m^{-2} s^{-1})	40.0	52.5	*; **
Water exchange				
GSmax	Maximum stomata conductivity (mmol H_2O m^{-2} s^{-1})	81.5	50.0	Medlyn and Jarvis (1999); Schumann et al. (2024)
GSmin	Minimum stomata conductivity (mmol H2O m^{-2} s^{-1})	4.3	2.0	*; **
H2OREF_GS	Relative available soil water content at which stomata closure starts	0.35	0.4	Granier et al. (2007); Granier et al. (2000)
WUECmax	Maximum water use efficiency (mg H_2O g C^{-1})	10.0	9.0	*; **
WUECmin	Minimum water use efficiency (mg H_2O g C^{-1})	7.0	6.0	*; **
Phenology				
DLEAFSHED	Total leaf longevity from emergence (days)	326	3180	*; **
GDDFOL-START	Temperature sum for foliage activity onset (°C)	346.9	155	*; **
MFOLpot	Foliage biomass for mature stands	0.25	1.2	*;

	under closed canopy condition (kg m^{-2})			**
NDFLUSH	Time interval necessary to complete flushing of foliage (days)	21	90	*; **
NDMORT	Time interval necessary to complete litterfall (days)	108	2815	*; **
SLAmax	Specific leaf area in the shade (m^2 kg^{-1})	31.0	7.5	Aranda et al. (2004); Bartelink (1996)
SLAmin	Specific leaf area in full light (m^2 kg^{-1})	11.0	3.5	Aranda et al. (2004); Bartelink (1996)
Others				
ALB	Foliage albedo	0.05	0.045	Dufrene et al. (2005); Hember et al. (2010)
EXT	Light extinction factor	0.532	0.453	Molina-Herrera et al. (2015); Raj et al. (2018)
KM20 (km20)	Maintenance coefficient at reference temperature	0.9	0.32	*; **
NCFOLopt	Optimum nitrogen concentration of foliage (%)	0.0254	0.015	Mellert and Göttlein (2012); Thom et al. (2024)

*defined from joined automated parametrization of a German (Leinefelde, DE-Lnf), a Danish (Soroe, DK-Sor), and a Czech (Stitna, CZ-Stn) site
**defined from joined automated parametrization of a site in Canada (Campbell River) and one from the Netherlands (Speulderbos)

References (Table S1)

Aranda, I., Pardo, F., Gil, L., and Pardos, J. A.: Anatomical basis of the change in leaf mass per area and nitrogen investment with relative irradiance within the canopy of eight temperate tree species, Acta Oecologica, 25, 187-195, 2004.

Bartelink, H. H.: Allometric relationships on biomass and needle area of Douglas-fir, Forest Ecol. Manage., 86, 193-203, 1996.

Dreyer, E., Le Roux, X., Montpied, P., Daudet, F. A., and Masson, F.: Temperature response of leaf photosynthetic capacity in seedlings from seven temperate tree species, Tree Physiol., 21, 223-232, https//doi.org/ 10.1093/treephys/21.4.223, 2001.

Dufrene, E., Davi, H., Francois, C., Le Maire, G., Le Dantec, V., and Granier, A.: Modelling carbon and water cycles in a beech forest Part I: Model description and uncertainty analysis on modelled NEE, Ecol. Modelling, 185, 407-436, https//doi.org/10.1016/j.ecolmodel.2005.01.004, 2005.

Falge, E., Ryel, R. J., Alsheimer, M., and Tenhunen, J. D.: Effects of stand structure and physiology on forest gas exchange: a simulation study for Norway spruce, Trees-Struct. Funct., 11, 436-448, 1997.

Granier, A., Loustau, D., and Bréda, N.: A generic model of forest canopy conductance dependent on climate, soil water availability and leaf area index, Annales des Sciences Forestieres, 57, 755-765, 2000.

Granier, A., Reichstein, M., Bréda, N., Janssens, I. A., Falge, E., Ciais, P., Grünwald, T., Aubinet, M., Berbigier, P., Bernhofer, C., Buchmann, N., Facini, O., Grassi, G., Heinesch, B., Ilvesniemi, H., Keronen, P., Knohl, A., Köstner, B., Lagergren, F., Lindroth, A., Longdoz, B., Loustau, D., Mateus, J., Montagnani, L., Nys, C., Moors, E., Papale, D., Peiffer, M., Pilegaard, K., Pita, G., Pumpanen, J., Rambal, S., Rebmann, C., Rodrigues, A., Seufert, G., Tenhunen, J., Vesala, T., and Wang, Q.: Evidence for soil water control on carbon and water dynamics in European forests during the extremely dry year: 2003, Agric. Forest Meteorol., 143, 123-145, 2007.

Hember, R. A., Coops, N. C., Black, T. A., and Guy, R. D.: Simulating gross primary production across a chronosequence of coastal Douglas-fir forest stands with a production efficiency model, Agric. Forest Meteorol., 150, 238-253, 2010.

Ibrom, A., Jarvis, P. G., Clement, R., Morgenstern, K., Oltchev, A., Medlyn, B. E., Wang, Y. P., Wingate, L., Moncrieff, J. B., and Gravenhorst, G.: A comparative analysis of simulated and observed photosynthetic CO_2 uptake in two coniferous forest canopies, Tree Physiol., 26, 845-864, 2006.

Kattge, J., and Knorr, W.: Temperature acclimation in a biochemical model of photosynthesis: a reanalysis of data from 36 species, Plant Cell Environ., 30, 1176-1190, https//doi.org/10.1111/j.1365-3040.2007.01690.x, 2007.

Long, S. P.: Modification of the response of photosynthetic productivity to rising temperature by atmospheric CO_2 concentrations: Has its importance been underestimated?, Plant Cell Environ., 14, 729-739, https//doi.org/10.1111/j.1365-3040.1991.tb01439.x, 1991.

Manter, D. K., Bond, B. J., Kavanagh, K. L., Stone, J. K., and Filp, G. M.: Modelling the impacts of the foliar pathogen, *Phaeocryptopus gaeumannii*, on Douglas-fir physiology: net canopy carbon assimilation, needle abscission and growth, Ecol. Modelling, 164, 211-226, 2003.

Medlyn, B. E., and Jarvis, P. G.: Design and use of a database of model parameters from elevated [CO_2] experiments, Ecol. Modelling, 124, 69-83, 1999.

Medlyn, B. E., Loustau, D., and Delzon, S.: Temperature response of parameters of a biochemically based model of photosynthesis. I. Seasonal changes in mature maritime pine (*Pinus pinaster* Ait.), Plant Cell Environ., 25, 1155-1165, 2002.

Mellert, K., and Göttlein, A.: Comparison of new foliar nutrient thresholds derived from van den Burg's literature compilation with established central European references, Eur. J. Forest Res., 131, 1461-1472, 2012.

Molina-Herrera, S., Grote, R., Santabárbara-Ruiz, I., Kraus, D., Klatt, S., Haas, E., Kiese, R., and Butterbach-Bahl, K.: Simulation of CO_2 fluxes at European forest ecosystems with the coupled soil-vegetation process model "LandscapeDNDC", Forests, 6, 1779-1809, https//doi.org/10.3390/f6061779, 2015.

Raj, R., Hamm, N. A. S., van der Tol, C., and Stein, A.: Bayesian integration of flux tower data into process-based simulator for quantifying uncertainty in simulated output, Geosci. Model Dev., 11, 83-101, https//doi.org/10.5194/gmd-11-83-2018, 2018.

Schumann, K., Schuldt, B., Fischer, M., Ammer, C., and Leuschner, C.: Xylem safety in relation to the stringency of plant water potential regulation of European beech, Norway spruce, and Douglas-fir trees during severe drought, Trees, 38, 607-623, https//doi.org/10.1007/s00468-024-02499-5, 2024.

Thom, D., Rammer, W., Albrich, K., Braziunas, K. H., Dobor, L., Dollinger, C., Hansen, W. D., Harvey, B. J., Hlásny, T., Hoecker, T. J., Honkaniemi, J., Keeton, W. S., Kobayashi, Y., Kruszka, S. S., Mori, A., Morris, J. E., Peters-Collaer, S., Ratajczak, Z., Simensen, T., Storms, I., Suzuki, K. F., Taylor, A. R., Turner, M. G., Willis, S., and Seidl, R.: Parameters of 150 temperate and boreal tree species and provenances for an individual-based forest landscape and disturbance model, Data in Brief, 55, 110662, https//doi.org/10.1016/j.dib.2024.110662, 2024.

Thornley, J. H. M.: Instantaneous canopy photosynthesis: Analytical expressions for sun and shade leaves based on exponential light decay down the canopy and an acclimated non-rectangular hyperbola for leaf photosynthesis, Ann. Bot., 89, 451-458, https//doi.org/10.1093/aob/mcf071, 2002.

Van Wijk, M. T., Dekker, S. C., Bouten, W., Bosveld, F. C., Kohsiek, W., Kramer, K., and Mohren, G. M. J.: Modeling daily gas exchange of a Douglas-fir forest: comparison of three stomatal conductance models with and without a soil water stress function, Tree Physiol., 20, 115-122, 2000.

Von Caemmerer, S., Evans, J. R., Hudson, G. S., and Andrews, T. J.: The kinetics of ribulose-1,5-bisphosphate carboxylase/oxygenase in vivo inferred from measurements of photosynthesis in leaves of transgenic tobacco, Planta, 195, 88–97, https//doi.org/10.1007/BF00206296, 1994.

Wang, Q., Tenhunen, J., Falge, E., Bernhofer, C., Granier, A., and Vesala, T.: Simulation and scaling of temporal variation in gross primary production for coniferous and deciduous temperate forests, Glob. Change Biol., 10, 37-51, https//doi.org/10.1111/j.1365-2486.2003.00716.x, 2003.

Warren, C. R., and Adams, M. A.: Internal conductance does not scale with photosynthetic capacity: implications for carbon isotope discrimination and the economics of water and nitrogen use in photosynthesis, Plant Cell Environ., 29, 192-201, 2006.

Yan, Y., Klosterhalfen, A., Moyano, F., Cuntz, M., Manning, A. C., and Knohl, A.: A modeling approach to investigate drivers, variability and uncertainties in O_2 fluxes and $O_2 : CO_2$ exchange ratios in a temperate forest, Biogeosciences, 20, 4087-4107, https//doi.org/10.5194/bg-20-4087-2023, 2023.